Developing Application Specific Semiconductor Imaging Modalities: High Resolution Neurological Imaging Using PET (Neuro-PET)

J. Smith[1], A. Groll[1], J. Kroeger[1], Ling-Jian Meng[1,2]
[1]Department of Nuclear, Plasma, and Radiological Engineering, [2] Beckman Institute, University of Illinois at Urbana-Champaign

INTRODUCTION

Neurodegenerative diseases such as Alzheimer's disease and Chronic Traumatic Encephalopathy (CTE) have become more prevalent in our population [1-2].The rise in penetrance and onset of these diseases has called for a more deliberate focus on understanding the pathology behind them. Alzheimer's and CTE are both characterized by the development of hyperphosphorylated Tau protein as well as Beta-Amyloid plaques and neurofibrillary tangles, metal cations have also been shown to play a role [3].

Our recent work has been on the development of an ultrahigh resolution hybrid pixel-waveform (HPWF) enabled CdTe semiconductor detectors for a PET-XRF imaging system. PET is well established for the imaging of the Tau protein as well as Beta-Amyloid plaques, whereas X-Ray fluorescence (XRF) is explored for potential integration of complimentary metal cation information within a body.

RESEARCH QUESTIONS

- What is the viable energy threshold of the system?
- How do characteristics such as amplitude and timing of the output signal waveforms influence resolution of the PET system?

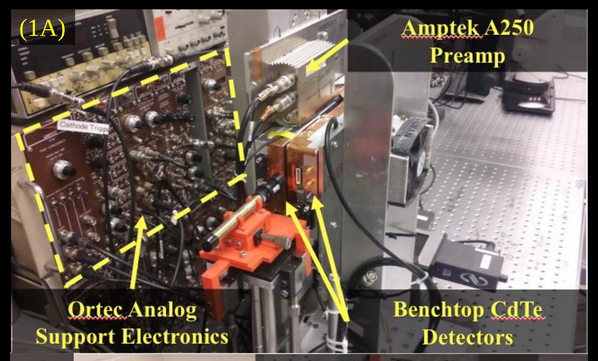

Fig. 1. (A) Ortec analog shaping and CFD electronics were used to process the Amptek A250 preamplifier signals generated from coincidence events. (B) System triggering is controlled by the FPGA coincidence control unit (Xilinx Spartan-3E). The 4-D stage used in the experiments allowed source alignment and the simulation of a multi-detector ring through rotation.

METHODS

- As compared to most PET systems that use scintillators in connection with photomultiplier tubes (PMT) we use a semiconductor CdTe detector
- This offers a direct conversion of interaction to signal and a high energy resolution [4]
- Our system consists of two CdTe detectors that have cathode and anode readouts (Figure 1)
- Signals are shaped with an NIM shaper and fed into a constant fraction discriminator, Ortec analog shaping and CFD electronics were used to process the Amptek A250 preamplifier signals, the pixel circuitry is working with a high-speed digitizer to sample the cathode waveform. (Figure 1)

Hybrid Pixel-Waveform CdTe Detectors

- Each hybrid is composed of a CdTe crystal with a pixelated anode bump-bonded to a 2048 (32 × 64)-channel Application Specific Integrated Circuit (ASIC) to read out the anode pixels
- Each pixelated element is 350 µm x 350 µm in size as shown in fig. 3. The CdTe hybrids are 2.2 cm wide and 1.1 cm long with a thickness of 2 mm.

Fig. 3. (A) Pixelated anode with each element sized as 350 µm x 350 µm. (B) 2 mm thick CdTe crystal added. (C) An 8 ASIC CdTe detector with the support electronics for reading out the anode. Not pictured are the preamplifier connection to the cathode. (D) Simplified schematic of anode and cathode signal readout information.

Cathode Waveform Physics and Fitting

◆**Electron-Hole Formation:** Upon photoelectric absorption, equal amounts of charge are formed

$$N_0 = N_e = N_h$$

◆**Electron-Hole Drifting Velocity:** The drifting velocity of electrons and holes differs greatly

$$v_e = \mu_e E = 10\, v_h = 10\, \mu_h E$$

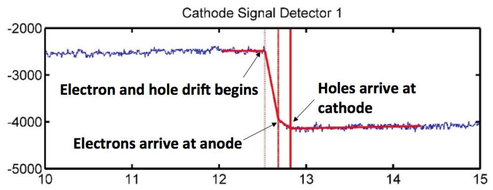

Fig. 4. (A) Digitized cathode from one of the detectors in the coincidence setup. The waveform is digitized and fitted using a linear fit method. Given the fitting it is possible to acquire the energy, depth of interaction and timing. The anode only provides the spatial position. x

RESULTS

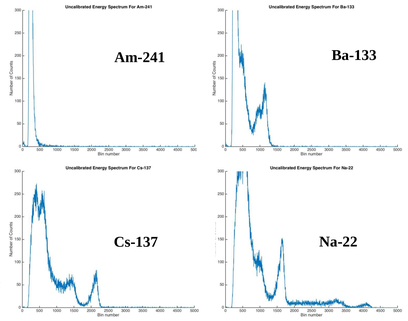

Fig. 5. Uncalibrated energy spectra for four different sources (from top left to bottom right) Am-241, Ba-133, Cs-137, and Na-22. These spectra were then used to create an energy calibration curve as shown in figure 6 where the 662 keV peak from Cs-137 along with the 511 keV and 1275 keV peak from Na-22 were used.

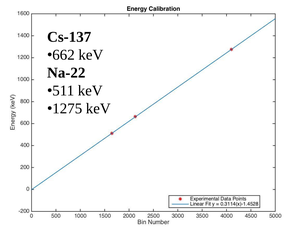

Fig. 6. Energy calibration curve for the four spectra. Three data points were used; the 662 keV peak from Cs-137, the 511 keV peak from Na-22, and the 1275 keV peak from Na-22. Applying this energy calibration curve from figure 6 we were then able to construct the calibrated energy spectra for the four sources as shown in figure 7 below.

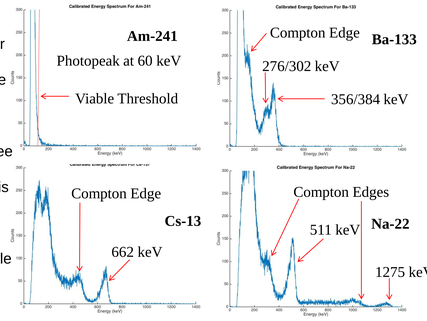

Fig. 7. The energy calibrated spectra for the four different sources. We are able to clearly define the photo-peaks and Compton edges for most sources. We see in the Am-241 spectrum that there is a viable energy threshold around 80keV. Peaks below this are not resolvable with this system.

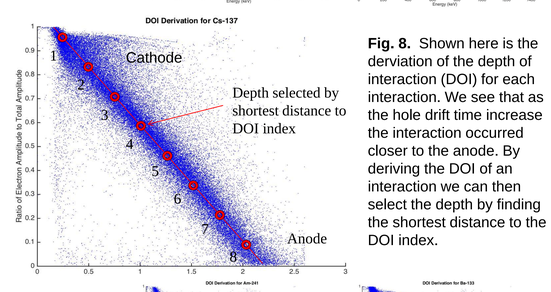

Fig. 8. Shown here is the derivation of the depth of interaction (DOI) for each interaction. We see that as the hole drift time increase the interaction occurred closer to the anode. By deriving the DOI of an interaction we can then select the depth by finding the shortest distance to the DOI index.

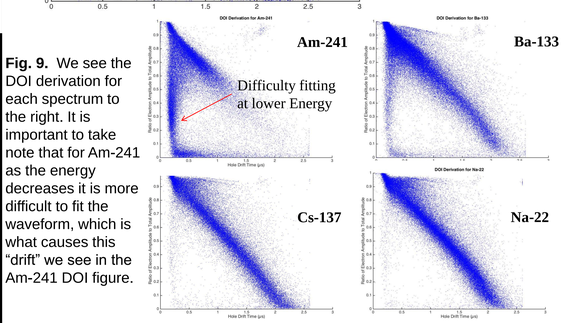

Fig. 9. We see the DOI derivation for each spectrum to the right. It is important to take note that for Am-241 as the energy decreases it is more difficult to fit the waveform, which is what causes this "drift" we see in the Am-241 DOI figure.

CONCLUSIONS

When considering this system for PET-XRF purposes we see that the viable resolution threshold is around 80 keV. We see that gold is the only biologically (therapeutically) relevant element with a k-edge around 80 keV. We also saw that for Na-22 with a 511 keV photopeak this system is able to resolve this photopeak very well. This means that the system is well established for PET processes but not so much for XRF imaging capabilities.

Atomic #/Element	K-edge (keV)
Os-76	73.869
Ir-77	76.111
Pt-78	78.400
Au-79	80.729
Hg-80	83.109
Tl-81	85.532
Pb-82	88.008
Bi-83	90.540
Po-84	93.113
At-85	95.730
Rn-86	98.402
Fr-87	101.131
Ra-88	103.909
Ac-89	106.738

Fig. 10. Chart of the k-edges around the resolvability determined for this system. The important element to take note of is Au-79 since it is biologically relevant and possible resolvable with our system [5].

FUTURE WORK

- Investigate the capacitive sensitivity of our readout electronics to try and push the energies past our noise threshold.
- Look at shaped spectra for minimal viable energy; the use of a shaping amplifier may allow us to increase our signal to noise ratio.

REFERENCES

[1] "Latest Alzheimer's Facts and Figures." *Latest Facts & Figures Report*. N.p., 17 Sept. 2013. Web. 25 Mar. 2016.
[2] "Study: 95.6 Percent of Deceased NFL Players Tested Positive for CTE."*CBSSports.com*. N.p., n.d. Web. 25 Mar. 2016.
[3] McKee, A. C., Stein, T. D., Kiernan, P. T. and Alvarez, V. E. (2015), The Neuropathology of Chronic Traumatic Encephalopathy. Brain Pathology, 25: 350–364. doi: 10.1111/bpa.12248
[4] Takahashi, Tadayuki, and Shin Watanabe. "Recent progress in CdTe and CdZnTe detectors." *IEEE Transactions on Nuclear Science* 48.4 (2001): 950-959.
[5] Kaye & Laby Tables of Physical & Chemical Constants. [Middlessex, England] :National Physical Laboratory, 2011. Print.

ACKNOWLEDGMENTS

I would like to say thank you to Andrew Groll, Jazz Kroeger, Ling-Jian Meng, and the University of Illinois for the opportunity to work on these projects.